Developmental Biology **216,** 595–610 (1999)
Article ID dbio.1999.9528, available online at http://www.idealibrary.com on IDEAL®

Locomotor Behavior, Vertebral Identity, and Peripheral Nervous System Development

Cecile C. de la Cruz, Andre Der-Avakian, Demetri D. Spyropoulos,* David D. Tieu, and Ellen M. Carpenter[1]

*Mental Retardation Research Center, Department of Psychiatry, University of California at Los Angeles School of Medicine, 48-228 NPI, 760 Westwood Plaza, Los Angeles, California 90024; and *Center for Molecular and Structural Biology, Hollings Cancer Center, Medical University of South Carolina, Room 334, 86 Jonathan Lucas Street, Charleston, South Carolina 29403*

The five most 5′ *HoxD* genes, which are related to the *Drosophila Abd-B* gene, play an important role in patterning axial and appendicular skeletal elements and the nervous system of developing vertebrate embryos. Three of these genes, *Hoxd11*, *Hoxd12*, and *Hoxd13*, act synergistically to pattern the hindlimb autopod. In this study, we examine the combined effects of two additional 5′ *HoxD* genes, *Hoxd9* and *Hoxd10*. Both of these genes are expressed posteriorly in overlapping domains in the developing neural tube and axial mesoderm as well as in developing limbs. Locomotor behavior in animals carrying a double mutation in these two genes was altered; these alterations included changes in gait, mobility, and adduction. Morphological analysis showed alterations in axial and appendicular skeletal structure, hindlimb peripheral nerve organization and projection, and distal hindlimb musculature. These morphological alterations are likely to provide the substrate for the observed alterations in locomotor behavior. The alterations observed in double-mutant mice are distinct from the phenotypes observed in mice carrying single mutations in either gene, but exhibit most of the features of both individual phenotypes. This suggests that the combined activity of two adjacent *Hox* genes provides more patterning information than activity of each gene alone. These observations support the idea that adjacent *Hox* genes with overlapping expression patterns may interact functionally to provide patterning information to the same regions of developing mouse embryos.

***Key Words:* *Hox* genes; vertebral transformation; patella; humerus; peripheral nerve.**

INTRODUCTION

The mouse genome contains 39 *Hox* genes which are related to the *Drosophila* homeotic genes and which encode transcription factors belonging to the *Antennepedia* class of homeodomain proteins. In the mouse, *Hox* genes are in four linkage groups positioned on four separate chromosomes. These four linkage groups are likely to have arisen by two duplications of an ancestral homeotic complex to produce four clusters of *Hox* genes in which individual genes within a cluster have one or more paralogues with highly conserved sequences and overlapping expression domains in the remaining clusters (reviewed in Rijli and Chambon, 1997). All *Hox* genes are expressed in broad axial domains during embryonic development with well-defined rostral boundaries and more diffuse caudal limits. Axial expression is evident in the developing central nervous system and adjacent somitic and unsegmented mesoderm. Genes within a single cluster are expressed in overlapping spatial domains which reflect their order on the chromosome with more 3′ genes expressed in more rostral domains and more 5′ genes expressed more caudally (Gaunt *et al.*, 1989; Izpisúa-Belmonte *et al.*, 1991). The temporal expression patterns of these genes also reflects their gene order within the linkage groups, with 3′ genes expressed earlier than 5′ genes. In addition to their axial expression, 16 of these

[1] To whom correspondence should be addressed at the Mental Retardation Research Center, Department of Psychiatry, UCLA School of Medicine, 48-228 NPI, 760 Westwood Plaza, Los Angeles, CA 90024. Fax: (310) 206-5050. E-mail: ecarpenter@mednet.ucla.edu.

0012-1606/99 $30.00

genes, which are related to the *Drosophila Abd-B* gene, are expressed in developing limb buds.

Mutational analysis in the mouse shows that *Hox* genes are required to establish the regional identity of a developing embryo. Disruption of *Hox* genes produces phenotypes characterized by alteration of positional identity affecting structures as diverse as the central nervous system, visceral organs, and skeleton. *Hox* genes provide patterning information for proper formation of hindbrain rhombomeres and motor nuclei (Carpenter *et al.,* 1993; Mark *et al.,* 1993; Goddard *et al.,* 1996), for specification of segmental identity in the spinal cord (Carpenter *et al.,* 1997; Tiret *et al.,* 1998), and for the formation and projection of spinal and peripheral nerves (Rancourt *et al.,* 1995; Rijli *et al.,* 1995; Tiret *et al.,* 1998). *Hox* genes also provide information for patterning the esophagus (Boulet and Capecchi, 1996) and reproductive tract (Satokata *et al.,* 1995; Bensen *et al.,* 1996) as well as for the generation and positioning of the bones of the axial and appendicular skeleton (Condie and Capecchi, 1993; Dollé *et al.,* 1993; Davis and Capecchi, 1994, 1996; Favier *et al.,* 1995, 1996; Fromental-Ramain *et al.,* 1996a,b). *Hox* genes may act independently (e.g., Bensen *et al.,* 1996; Boulet and Capecchi, 1996; Carpenter *et al.,* 1993, 1997; Davis and Capecchi, 1994; Satokata *et al.,* 1995) or in combination with one another (e.g., Condie and Capecchi, 1994; Davis and Capecchi, 1996; Davis *et al.,* 1995; Gavalas *et al.,* 1998; Rancourt *et al.,* 1995; Studer *et al.,* 1998) during embryonic development. These observations suggest that *Hox* genes are required independently and in combination with one another to pattern developing embryos.

Mutations in single *Hox* genes produce phenotypes which are typically restricted to a small portion of the gene expression domain, with the predominant phenotypes affecting structures at or near the anterior limit of expression. Mutations in two or more adjacent, paralogous, or similarly expressed *Hox* genes combine to produce more widespread effects, often unmasking phenotypes not evident following single mutation of any of the genes involved. These observations suggest functional redundancy among the *Hox* genes, such that inactivation of one gene can be compensated by the activity of other *Hox* genes which share sequences or have similar domains of expression. Inactivation of three members of the *HoxD* family, *Hoxd11, Hoxd12,* and *Hoxd13,* which are expressed in overlapping domains, individually produced subtle phenotypes affecting digit formation (Davis and Capecchi, 1994, 1996). *Trans*-heterozygotes which combined mutations in either *Hoxd11* or *Hoxd12* with a mutation in *Hoxd13* produced more severe digit phenotypes (Davis and Capecchi, 1996). Deletion of all three genes together revealed additional phenotypes (Zákány and Duboule, 1996). All of these observations suggest functional interactions between members of the same linkage group.

We have addressed the combined function of two additional 5′ members of the *HoxD* family, *Hoxd9* and *Hoxd10.* These two genes are expressed in more rostral axial domains than *Hoxd11, Hoxd12,* and *Hoxd13* and are also expressed more proximally within the developing limb buds (Dollé *et al.,* 1989). Mutations in these genes individually produce skeletal defects affecting lumbar and sacral vertebrae, the stylopod and proximal zeugopod in the forelimbs and hindlimbs, and alterations in lumbar spinal cord patterning (Carpenter *et al.,* 1997; Fromental-Ramain *et al.,* 1996a). In this study, these genes were simultaneously disrupted by introduction of a *neo* resistance gene into *Hoxd9* and a frameshift mutation into *Hoxd10.* Our observations suggest that the double mutation predominantly affects the areas of the skeleton and central nervous system affected by single mutations in *Hoxd9* or *Hoxd10* but also demonstrates some unmasking of phenotypes not evident in the single mutant mice. These observations support the idea that interactions between members of the same linkage group are required for proper patterning of the developing mouse embryo.

METHODS AND MATERIALS

Gene Targeting

A 10-kb genomic DNA fragment containing both *Hoxd9* and *Hoxd10* sequences was isolated from a 129Sv library in Lambda FIX II (Stratagene) and used as the basis for a replacement-type gene targeting vector. The targeting vector, composed of the isolated and modified genomic sequence flanked by two thymidine kinase genes, was constructed in a pUC plasmid. *Hoxd9* was inactivated by insertion of a pMC1*neo*-poly(A) cassette (Thomas and Capecchi, 1987) in the forward orientation into an *Eco*47III restriction enzyme site in the second exon. This site corresponds to the position of amino acid 4 in the homeodomain (Renucci *et al.,* 1992). *Hoxd10* was inactivated by insertion of an 8-bp *Eco*RI linker into a *Hpa*I site in the second exon of *Hoxd10.* This site corresponds to the position of amino acid 38 in the second α-helix of the homeodomain (Renucci *et al.,* 1992). The targeting construct was electroporated into CC1.2 ES cells and targeted clones were selected by positive/negative selection as described (Mansour *et al.,* 1988). Correct integration of the targeting vector was verified by enzymatic digestion using *Eco*RI or *Eco*RV and Southern blotting using both 3′ and 5′ flanking probes (data not shown). Hybridization with a *neo*-specific probe confirmed the integrity of the targeting event. Three of 192 cell lines screened tested positive for insertion of both mutations; one additional cell line contained the linker alone. Correctly targeted ES cells were injected into C56Bl/6J (B6) blastocysts to produce chimeric mice which transmitted the mutation through their germ line as described (Thomas and Capecchi, 1990). Mutant mice were initially screened by Southern blotting using flanking probes to detect both mutations; subsequent generations were screened by PCR using the primers D9 forward, 5′-AGC GAA CTG GAT CCA CGC TCG CTC CA-3′; D9 reverse, 5′-GAC TTG TCT CTC TGT AAG GTT CAG AAT CC-3′; and *neo* reverse, 5′-CGT GTT CGA ATT CGC CAA TGA CAA GAC-3′; which produce a wild-type band of 160 bp and a mutant band of 264 bp. Because of the close proximity of the two mutations in the genome, animals which carry the *Hoxd9* mutation identified by PCR should also carry the linker insertion mutation in *Hoxd10.* Confirmation of transmission of the mutation in *Hoxd10* was made by amplifying exon 2 sequences using D10 forward primer 5′-GAA GAG GTG CCC TTA CAC CA-3′ and D10 reverse primer 5′-TCG ATT CTC

TCG GCT CAT CT-3′ and subjecting amplified fragments to digestion with *Eco*RI to detect the presence of the linker insertion.

The mutation was maintained on a hybrid 129Sv/B6 background. Control and mutant animals used for experiments were produced by intercrossing heterozygous parents; littermates were collected as embryos or adults for further analysis.

Footprint Patterns

Wild-type and *Hoxd9/Hoxd10* mutant mice were trained to walk through a 24 × 3-in. open-top tunnel. Once training was completed, the ventral surfaces of the hindfeet were painted with nontoxic tempera paint and the mice walked through the tunnel for four consecutive trials to record footprints. Patterns of locomotion were examined by measuring the angles of hindfoot placement relative to the direction of motion, the average distance between prints, and the presence and number of foot drags. Data from wild-type and mutant animals were collated, pooled, and examined for statistical significance using a two-sample Student *t* test assuming unequal variances.

Locomotion and Adduction

Locomotor behavior was examined using a modified open field paradigm. Individual adult mice were placed in the center of a 12 × 18-in. observation chamber sectioned into quadrants and scored for the number of quadrants entered in a 5-min trial. Scores for individual mice were averaged, then scores for wild-type and mutant mice were pooled and averaged. Animals were also scored for the number of unsupported rearings onto their hindlimbs during the same trial. Each mouse was tested three times with a minimum delay of 2 days in between each trial. One male mutant mouse did not complete its third trial. Alterations in gait and adduction were identified and scored as previously described (Carpenter *et al.*, 1997).

Skeletal Analysis

Skeletons of wild-type and mutant adult mice were prepared and examined as described (Mansour *et al.*, 1993). Skeletons were observed for structural alterations in sacral and lumbar vertebrae and for alterations in forelimb and hindlimb structure.

Whole-Mount Immunohistochemistry

Embryos were collected at E12.5 and prepared for whole-mount immunohistochemistry as previously described (Carpenter *et al.*, 1997) with minor modification. 2H3 antibody supernatant (Developmental Studies Hybridoma Bank) was used at a dilution of 1:10 in PBSTMD (1% Tween 20, 2% skim milk powder, 1% dimethyl sulfoxide in PBS); embryos were incubated in primary antibody for 3 to 5 days. HRP-conjugated donkey anti-mouse antibody (1:200; Jackson Immunoresearch) was used as a secondary antibody; HRP reaction product was detected with 0.003% H_2O_2 in 1 mg/ml DAB in PBS plus 1% Tween 20 (PBST). When the desired intensity was attained, embryos were washed with PBST, rinsed in 5% acetic acid/70% methanol for 1 h, dehydrated in 100% MeOH, and cleared in 1:2 benzyl alcohol:benzyl benzoate. Embryos were transected below the forelimbs, mounted on chambered glass slides, and photographed using a Zeiss SV-11 stereomicroscope. Measurements were taken using an objective micrometer.

Carbocyanine Dye Tracing

Embryos were collected at E13.5, pinned, and fixed as described (Carpenter *et al.*, 1997). To label the lumbar nerve roots and the sacral plexus, dye injections were made with a picospritzer (General Valve) at the base of the hindlimb using a 1% solution of DiI (Molecular Probes) in dimethyl formamide. Dye transport, evisceration, and dissection were performed as described (Carpenter *et al.*, 1997). Embryos were initially examined using a Zeiss Axioscope with incident-light fluorescence then analyzed using a Bio-Rad MRC-600 confocal microscope. Confocal images were collected as a *Z* series at 3-μm intervals and merged to a single frame for further analysis.

RESULTS

Hoxd9 and Hoxd10 Are Disrupted by Gene Targeting

Hoxd9 and *Hoxd10* were simultaneously disrupted by gene targeting in ES cells. For the targeting vector, a 10-kb genomic DNA fragment containing coding sequences for *Hoxd9* and *Hoxd10* was cloned and modified such that the *neomycin resistance* gene was inserted into the second exon of *Hoxd9* and an *Eco*RI linker was inserted into the second exon of *Hoxd10*. The resulting genomic DNA structure is illustrated in Fig. 1A. The *neo* insertion into *Hoxd9* occurs near the N-terminal end of the homeodomain, at the position of amino acid 4 (Renucci *et al.*, 1992). This insertion should interfere with protein function by interruption of the amino acid sequence encoded by most of exon 2, effectively eliminating the activity of the homeodomain. The linker insertion into *Hoxd10* is positioned at the C-terminal end of second α-helix of the homeodomain (Renucci *et al.*, 1992; Bürglin, 1994). This insertion produces a frameshift which alters the identity of all amino acids downstream of the insertion and introduces a stop codon 57 bases downstream of the insertion site, terminating the protein 19 amino acids after the insertion site. This frameshift alters and prematurely terminates the coding sequence for the third α-helix, which should interrupt major groove contacts to DNA and interfere with intramolecular contacts primarily with the first α-helix (Bürglin, 1994). These two mutations together are likely to significantly disrupt the activity of both *Hoxd9* and *Hoxd10*.

Hoxd9/Hoxd10 animals are genotyped using PCR with primers positioned around the *neo* gene insertion in exon 2 of *Hoxd9*. These primers produce a wild-type band at 160 bp and a mutant band at 264 bp (Fig. 1B). *Hoxd9* and *Hoxd10* are separated by fewer than 4 kb on mouse chromosome 2 (Renucci *et al.*, 1992), making the likelihood of cotransfer very high, so identification of the *Hoxd9* mutation is used to predict the presence of the double mutation. Heterozygous animals appear phenotypically normal and did not present any behavioral alterations (Table 1, see below). Mutant animals are produced in the expected Mendelian ratio from intercrosses of heterozygous parents and are viable to weaning and adulthood. Mutant females are fertile

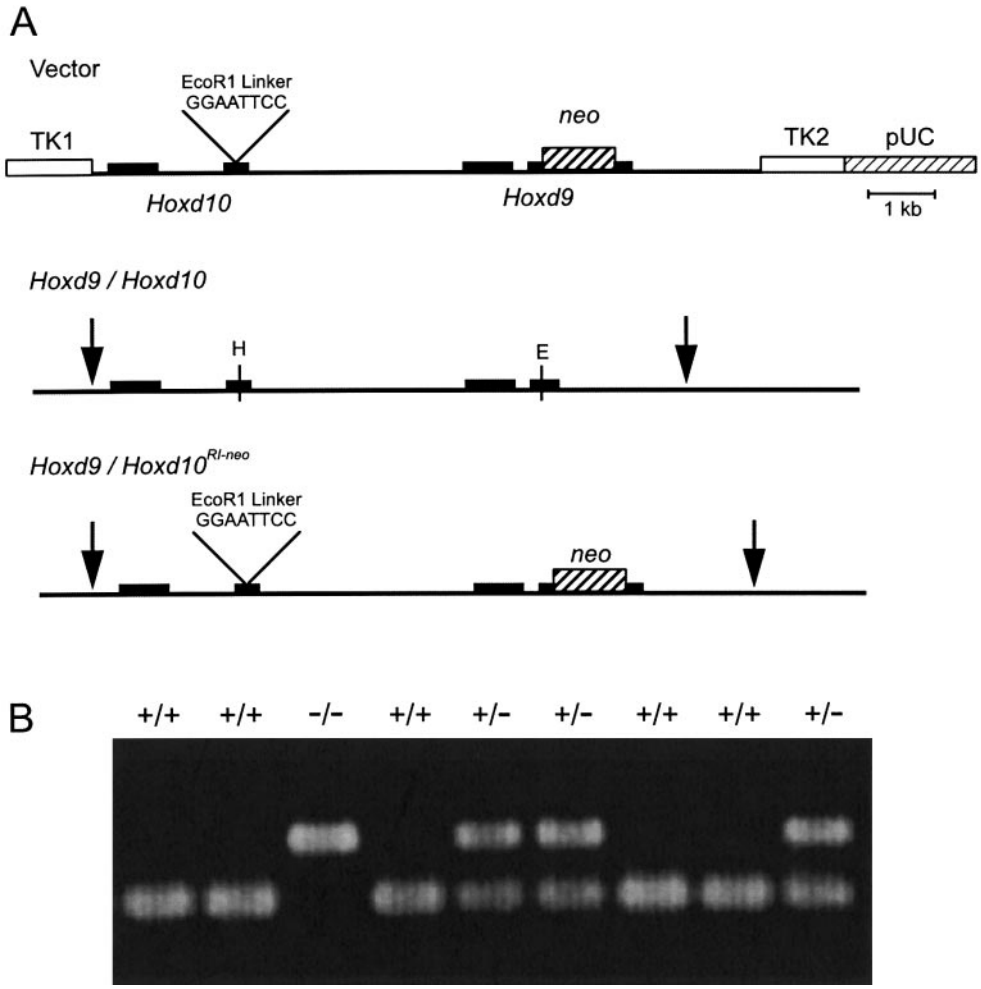

FIG. 1. Targeted mutagenesis of *Hoxd9/Hoxd10* and genotype analysis. (A) Illustration of the targeting vector (upper line), organization of the wild-type *Hoxd9/Hoxd10* locus (middle line), and arrangement of the *Hoxd9/Hoxd10* region after gene targeting (lower line). *Hoxd9* and *Hoxd10* exons are depicted by black boxes; the *neo* cassette disrupts exon 2 of *Hoxd9* at the *Eco*47III site (E), and an *Eco*RI linker disrupts exon 2 of *Hoxd10* at the *Hpa*I site (H). The white boxes are the *thymidine kinase* genes TK1 and TK2 and the plasmid vector backbone is labeled pUC. The vertical arrows represent the extent of the genomic DNA used to construct the targeting vector. (B) *Hoxd9/Hoxd10* animals were genotyped using PCR with primers positioned around and in the *neo* gene insertion in *Hoxd9* to produce a wild-type band at 162 bp and a mutant band at 264 bp. Genotypes for a single litter of pups produced from heterozygous parents are illustrated.

as judged by frequency of vaginal plugging and subsequent generation of embryos. Occasionally, females were observed to have difficulty in delivering full-term offspring, usually resulting in the death of the mother; however, abnormalities in uterine structure or position were not observed in mutant females. Mutant males are sterile with 100% penetrance; males are unable to induce vaginal plugs or pregnancies in females. Male sterility does not result from alterations in production of sperm or from anatomical abnormalities affecting the testes, epididymis, or ductus deferens (data not shown). Male sterility may result from operational impairment due to the hindlimb defects described below.

Locomotor Behavior Is Altered in Hoxd9/Hoxd10 Mutant Mice

Mutant mice were examined for alterations in gait, adduction, mobility, and weight-bearing ability. Alterations in all four behaviors were observed in mutant animals. Locomotor behavior was assayed by analyzing footprints collected from mice walking through a open-top tunnel (Figs. 2A–2C). Wild-type mice position their feet nearly in line with the direction of motion and balance their weight almost exclusively on the toes and the ball of the foot (Fig. 2A). In contrast, mutant mice position their feet outward, generating a large angle between their foot position and

TABLE 1

Presence of Alterations in Gait and Adduction in *Hoxd9/Hoxd10* Mutant Mice

Genotype	No gait defect	Mild gait defects	Severe gait defects	Adduction defect
+/+	14/14	0/14	0/14	0/14
+/−	19/19	0/19	0/19	0/19
−/−	4/17	11/17	2/17	12/17[a]

Note. Mild gait defects: jerky gait, slight hindlimb stiffness, abnormal foot posture. Severe gait defects: pronounced hindlimb stiffness, abnormal posterior hindlimb extension, improper weight distribution on dorsal surface of foot. Adduction defect: inability to bring hindlimbs together along ventral midline.

[a] Adduction was abnormally difficult in the five mutant animals that were able to bring their hindlimbs together on the midline.

their direction of motion (Figs. 2B and 2F). In addition, mutant mice distribute their weight more uniformly over the entire lower surface of their feet. The stride length of mutant mice is significantly shorter than wild-type controls; this disparity increases slightly with increasing age of the animal (Fig. 2G). Mutant mice also drag their feet during locomotion, as judged by visual observation during locomotion and by the presence of paint streaks between adjacent footprints (Fig. 2C). Foot-dragging behavior was never observed in wild-type animals.

Mobility was examined in mutant mice using a modified open-field paradigm. Mice were introduced into a chamber divided into quadrants and scored for the number of quadrants entered during a 5-min trial. On average, mutant animals entered significantly fewer quadrants than did wild-type controls (Fig. 2D, $P < 0.001$). During the open field trials, animals were also observed for their ability to stand upright on their hindlimbs without support from the walls of the chamber, which is a natural exploratory behavior of the mouse. Mutant mice stood upright far less frequently than did wild-type controls (Fig. 2E, $P < 0.05$). Taken together, these observations suggest significant alterations in the mobility of *Hoxd9/Hoxd10* mutant mice.

Gait defects were scored by observation as mild or severe (Table 1), with mild defects consisting of increased hindlimb stiffness, jerky gait, and abnormal outward positioning of the hindfeet and severe defects including pronounced hindlimb stiffness, abnormal posterior hindlimb extension, and improper weight distribution such that the hindfoot was turned over and the dorsal surface of the foot used as a weight-bearing surface. Twenty-three percent of mutant mice examined demonstrated normal gait, while 65% had mild gait defects and 12% had severe gait defects (Table 1). Gait defects were not observed in wild-type or heterozygous mice (Table 1). Defects in adduction were determined by scoring the ability of the animals to grasp an object presented along their ventral midline with their hindlimbs. Alterations in adduction were observed in all mutant mice examined. Seventy percent of mutant animals were unable to bring their hindlimbs together to grasp the midline object. The remaining 30% of animals were able to bring their hindlimbs together to grasp an object, but adduction appeared very difficult, with considerable muscle strain as judged by the presence of hindlimb muscle spasms during grasping. Similar spasms were never seen in wild-type or heterozygous animals.

Skeletal Alterations

Skeletons were prepared from adult mice and stained using alizarin red. Previous observations on mice carrying single mutations in either *Hoxd9* or *Hoxd10* have demonstrated that lumbar and sacral vertebrae are altered (Fromental-Ramain *et al.,* 1996a; Carpenter *et al.,* 1997), so the vertebral column was examined for evidence of vertebral transformation. In wild-type mice, there are four sacral vertebrae (S1–S4, Fig. 3A). S1 and S2 have expanded, wing-shaped transverse processes, S3 has a transitional shape midway between the shapes of S2 and S4, and S4 has smooth anterolaterally directed transverse processes. S1–S3 are normally fused at the tips of their transverse processes, while S4 remains free. In addition, S1 articulates with the ilium to anchor the vertebral column to the pelvis. *Hoxd9/Hoxd10* mutant mice show anterior transformation of sacral vertebrae such that 31 of the 41 mutants examined appear to have an additional S1 vertebrae (Figs. 3B and 3C; designated S1* following the nomenclature established in Fromental-Ramain *et al.,* 1996a) as judged by a secondary articulation of this vertebra to the ilium. Shape changes in the transverse processes of more posterior sacral vertebrae produce additional vertebrae with wing-shaped transverse processes (Table 2). In all mutant animals examined, the vertebrae occupying the wild-type S3 position have wing-shaped transverse processes, suggesting that the S3 vertebra in *Hoxd9/Hoxd10* mutant animals is transformed to an S2 (Figs. 3B and 3C; designated S2*). Two mutant animals have four sacral vertebrae with wing-shaped transverse processes, suggesting further anterior transformation in a small percentage of mutant animals. There is also additional fusion of transverse processes, such that 25 of 41 mutant animals have four fused sacral vertebrae (Figs. 3B and 3C; Table 2), rather than three fused vertebrae, as is seen in wild-type animals. These changes reflect transformations similar to those observed in *Hoxd9* and *Hoxd10* mutant animals (Carpenter *et al.,* 1997; Fromental-Ramain *et al.,* 1996a).

Observations on *Hoxd9* mutant animals have also identified alterations in the lumbar vertebrae, particularly in the shape and position of the spinous processes (Fromental-Ramain *et al.,* 1996a). Eighteen *Hoxd9/Hoxd10* mutants were examined for similar lumbar vertebral alterations. No consistent lumbar vertebral alterations were observed in *Hoxd9/Hoxd10* mutants, suggesting that the sacral transformations described above predominate in the double mutant.

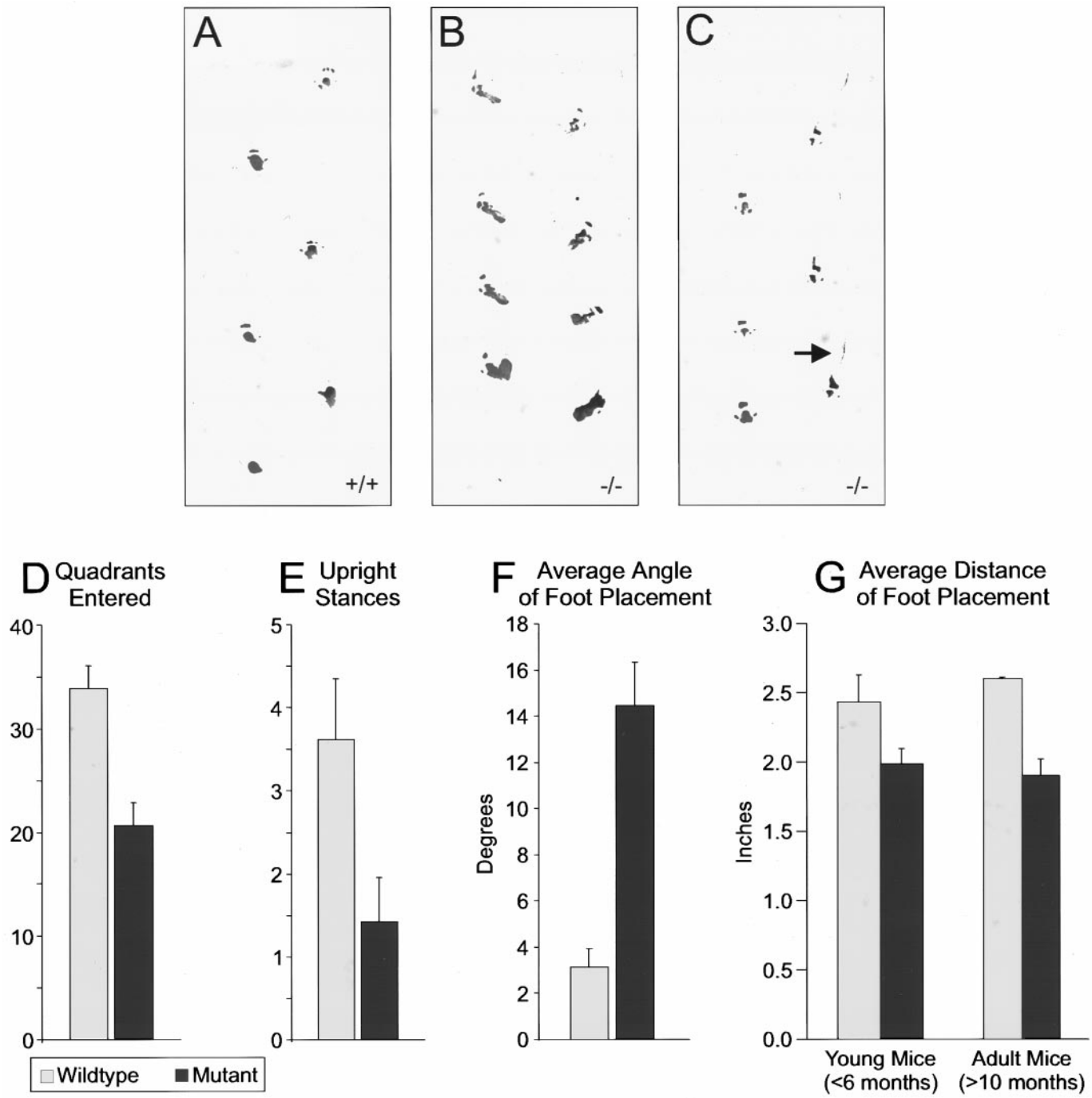

FIG. 2. Footprint patterns and behavioral testing show alterations in locomotor behavior in *Hoxd9/Hoxd10* mutant mice. Footprints taken from wild-type control (A) and mutant (B and C) mice were analyzed for foot placement, spacing, and drag. (A) Wild-type mice positioned their feet parallel to the linear direction of motion and distributed their weight on the ball of the foot and toes. (B) *Hoxd9/Hoxd10* mutant mice positioned their feet outward and distributed their weight on the entire ventral surface of the hindfoot. (C) Mutant mice also dragged their feet between footprints (arrow). (D) Mutant ($n = 16$) and wild-type ($n = 14$) mice were scored for the number of quadrants entered in a 12 × 18-in. observation chamber during three separate 5-min trials. Mutant mice entered significantly fewer quadrants than wild-type controls ($P \leq 0.001$). Statistical significance of the changes in D as well as in E–G was determined using a two-sample Student t test assuming unequal variances. (E) Mutant mice ($n = 16$) stood upright significantly fewer times than did wild-type controls ($n = 14$; $P \leq 0.01$). (F) Footprint analysis in mutant mice ($n = 10$) demonstrated a significantly ($P \leq 0.001$) greater angle outward away from the linear direction of motion compared to wild-type control mice ($n = 10$). (G) Spacing between footprints is shorter in mutant animals ($n = 10$) compared to wild-type controls ($n = 10$). Print spacing showed greater decreases in older animals ($P \leq 0.001$) compared with younger animals ($P \leq 0.05$).

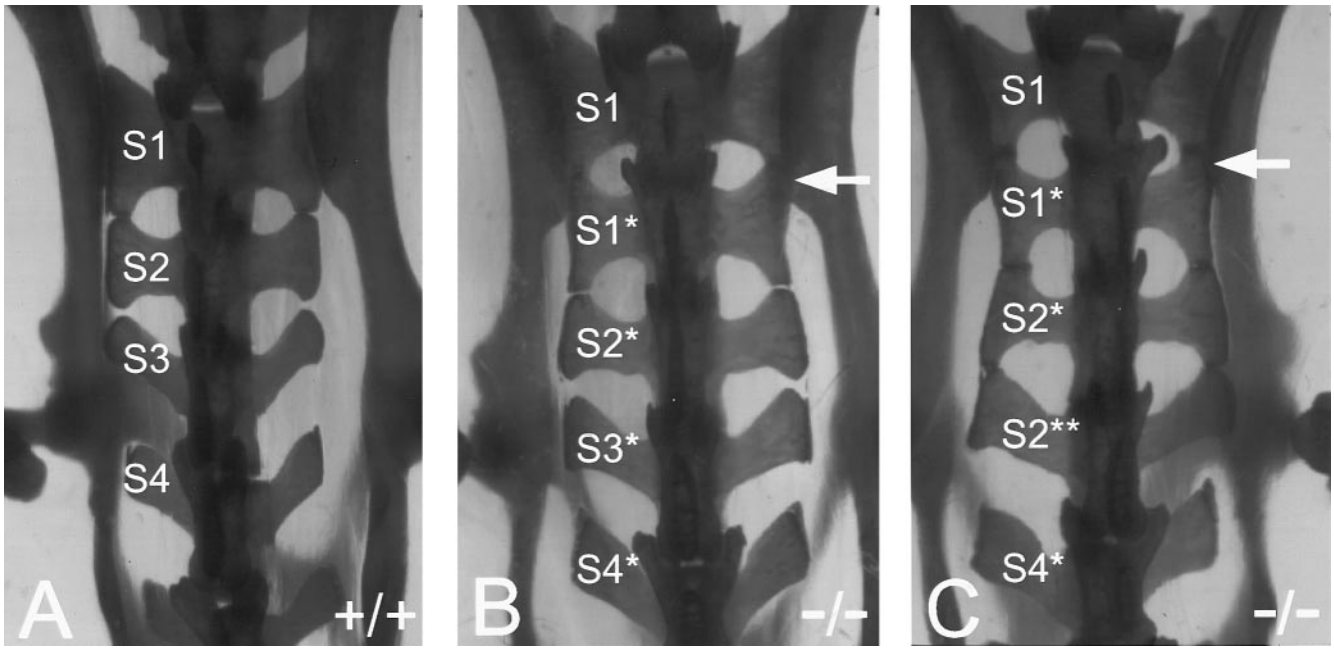

FIG. 3. Alterations in sacral vertebrae in *Hoxd9/Hoxd10* mutant mice. (A) Adult wild-type mice have four sacral vertebrae (S1–S4). (B and C) *Hoxd9/Hoxd10* mutant mice show anterior transformation of sacral vertebrae. Transformed vertebrae are indicated with asterisks. 75% of mutant animals show transformation of S2 into an S1-like phenotype (S1*). In these animals, S1* has a secondary articulation to the ilium (arrows) and pronounced wing-shaped transverse processes. More caudal vertebrae shift their identities such that they adopt the phenotype of the next most anterior vertebra (S2*, S3*, and S4* in B and C), producing five sacral vertebrae in mutant animals. Transformations are occasionally observed in more caudal vertebrae, producing duplications of additional vertebrae (S2** in C). Sacral vertebrae have shifted with respect to the position of the ilium such that the fourth sacral vertebra (S3* in B or S2** in C) now lies opposite the point of articulation between the pelvis and the femur.

Alterations were also observed in hindlimb and forelimb bones (Figs. 4 and 5; Table 2). In hindlimbs, the articulation point between femur and tibia was shifted in 27% of mutant hindlimbs, producing an outward rotation of the lower part of the limb (Figs. 4A–4C). In addition, the spacing between femur and tibia appeared expanded in mutants, suggesting an instability of the joint (Figs. 4D and 4E). The patella was shifted proximally along the femur in 74% of mutant hindlimbs such that it was positioned proximal to the lateral epicondyle, rather than adjacent to the epicondyle as is seen in wild-type animals (Figs. 4D, 4E, 4G, and 4H). The shape of the patella varied from smooth and oval to highly irregular in mutant animals. In some cases, the patella appeared to be composed of several parts (Fig. 4F), similar to the fragmented sesamoid bones produced in *Hoxa9/Hoxd9* double mutants (Fromental-Ramain *et al.*, 1996a). Small ectopic anterior sesamoid bones were produced proximal to the patella in 32% of mutant hindlimbs (Fig. 4H, Table 2). Some of these alterations were also observed in wild-type hindlimbs, but with a lesser degree of severity and at significantly lower frequency (Table 2). Most of these alterations are similar to alterations observed in the hindlimb of *Hoxd10* mutant animals (Carpenter *et al.*, 1997).

Inactivation of *Hoxd9* alone produces subtle alterations in the humerus, including an 8–10% reduction in length and the presence of an underdeveloped deltoid crest (Fromental-Ramain *et al.*, 1996a). Combining a *Hoxd9* mutation with a mutation in *Hoxa9* produces a flattened humeral head and the presence of extra or ectopic lateral, medial, or ventral sesamoid bones in the elbow joint (Fromental-Ramain *et al.*, 1996a). Eleven percent of *Hoxd9/Hoxd10* mutants have a flattened humeral head (Figs. 5A and 5B, Table 2) and 13% of mutants show alterations in the deltoid crest such that the slope of the crest begins more distally than normal and the size of the crest is somewhat reduced (Fig. 5B, Table 2). These alterations resemble the reported deltoid crest alterations in *Hoxd9* mutants. Some *Hoxd9/Hoxd10* mutants also have ectopic lateral sesamoid bones (Table 2), similar to those reported for *Hoxa9/Hoxd9* mutants. One forelimb alteration present in *Hoxd9/Hoxd10* mutant animals which is not seen in *Hoxd9* single-mutant animals is the production of an ectopic sesamoid bone on the dorsal aspect of the limb (Fig. 5D, Table 2). This sesamoid bone appears in 17% of *Hoxd9/Hoxd10* mutants and is curved around the base of the humerus opposite the position of the orthotopic sesamoid bone present on the ventral side of the forelimb. Ectopic

TABLE 2
Presence of Skeletal Alterations in *Hoxd9/Hoxd10* Mutant Mice

	Genotype	
	+/+	−/−
(A) Alterations in sacral vertebrae		
Transverse process fusion		
S1 → S2	11/15	41/41
S2 → S3	4/15	35/41
S3 → S4	0/15	25/41
S2 articulates to ilium	0/15	31/41
Wing-shaped transverse processes on S3	1/15	41/41[a]
(B) Appendicular skeletal alterations		
Hindlimb skeletal alterations		
Shift in articulation between femur and tibia	1/30	20/74
Rotation of tibia	1/30	19/74
Proximal shift of patella	5/30	55/74
Ectopic anterior sesamoid	4/30	24/74
Forelimb skeletal alterations		
Flattened humeral head	0/30	5/46
Underdeveloped deltoid crest	0/30	6/46
Supernumerary lateral sesamoid bone	0/30	8/46
Ectopic dorsal sesamoid bone	0/30	8/46

[a] Includes two mutants in which both S3 and S4 had wing-shaped transverse processes.

sesamoid bones have been reported in *Hoxa9/Hoxd9* double mutants (Fromental-Ramain *et al.*, 1996a), but not in the dorsal position.

Nervous System Alterations

Hoxd9/Hoxd10 mutant animals were examined for the presence of nervous system alterations using anti-neurofilament immunohistochemistry (Fig. 6) and carbocyanine dye tracing (Fig. 7). In wild-type animals at E12.5, hindlimb nerves stemming from both the lumbar and the sciatic plexus are well differentiated and nerves emerging from the sciatic plexus have grown approximately two-thirds the length of the hindlimb (Fig. 6A). Carbocyanine dye injections made immediately distal to the sciatic plexus retrogradely label three to four spinal nerves in both wild-type and mutant embryos (Figs. 7A and 7B). In wild-type embryos, three spinal segmental nerves, L3–L5, have robust projections through the sciatic plexus, with a smaller and more variable projection from L6 (Fig. 7A). In mutant embryos, the L3 projection is greatly reduced, while the projections from L4 to L6 appear similar to those seen in wild-type controls (Fig. 7B). The sciatic nerve is the major nerve emerging from the sciatic plexus; distal to the plexus, this nerve branches into the tibial and peroneal nerves. The tibial nerve provides innervation for plantar flexion and inversion of the foot and plantar flexion of the toes. The peroneal nerve divides into superficial and deep branches and innervates the knee joint, the skin of the calf and dorsal foot, and the anterolateral extensor muscles of the leg. On the medial face of the wild-type mouse hindlimb at E12.5, the tibial nerve terminates in an elaborate planar arbor which will subsequently divide into five branches to provide innervation for the plantar muscles of the toes (Fig. 6A). In 36% of mutant embryos, the tibial nerve is truncated and the distal arbor is missing (Fig. 6B). In other embryos, the tibial nerve appears to have extended normally, but the arbor appears more disorganized with fewer nerve fibers and fewer well-defined nerve branches. Carbocyanine dye tracing also demonstrates alterations in the tibial nerve arbor. By E13.5 in wild-type embryos, the tibial nerve arbor can be observed roughly dividing into five major branches (Figs. 7C and 7D). Nerve fibers are bundled together into thick fascicles within the body of the arbor, while individual fibers remain dispersed at the distal end of the arbor. This distal behavior is suggestive of pathfinding behavior demonstrated by growth cones at choice points in the chick limb (Tang *et al.*, 1994). In mutant embryos, fibers in the tibial nerve arbor remain dispersed, with little indication of bundling into identifiable fascicles (Figs. 7E, 7F, and 7G). Truncation of the tibial arbor is also evident in a few embryos at this stage (Fig. 7H), suggesting that the truncation observed in anti-neurofilament-labeled embryos was not simply due to a delay in development.

The deep branch of the peroneal nerve also shows alterations in *Hoxd9/Hoxd10* mutant embryos. The developing peroneal nerve normally projects through the hindlimb more dorsally than the tibial nerve and branches into the superficial and deep peroneal nerves at the level of the knee. In wild-type embryos, just posterior to the division into superficial and deep branches, the peroneal nerve (Fig. 6C) averages 39 μm in diameter, with a range of 20–50 μm (n = 14). At the same position in mutant embryos (Fig. 6D), the peroneal nerve averages 23 μm in diameter, with a range of 10–30 μm (n = 19), corresponding to an average 40% reduction in nerve diameter. Similar alterations in the tibial or peroneal nerves were never observed in wild-type or heterozygous embryos.

Gross dissection of adult hindlimbs also revealed abnormalities in peripheral nerve projections (Table 3). The presence or absence of five major nerve trunks was scored in 6 wild-type and 18 mutant hindlimbs. The common peroneal nerve was missing in 1 hindlimb and significantly reduced in 10 additional hindlimbs and the tibial nerve was reduced in 2 hindlimbs. These observations reflect the continued presence of altered peripheral nerve projections in adult mutant mice.

Other Alterations

Distal limb musculature was dissected in 6 wild-type and 18 *Hoxd9/Hoxd10* mutant adult hindlimbs. Limbs were scored for the presence or absence of 11 muscles in three

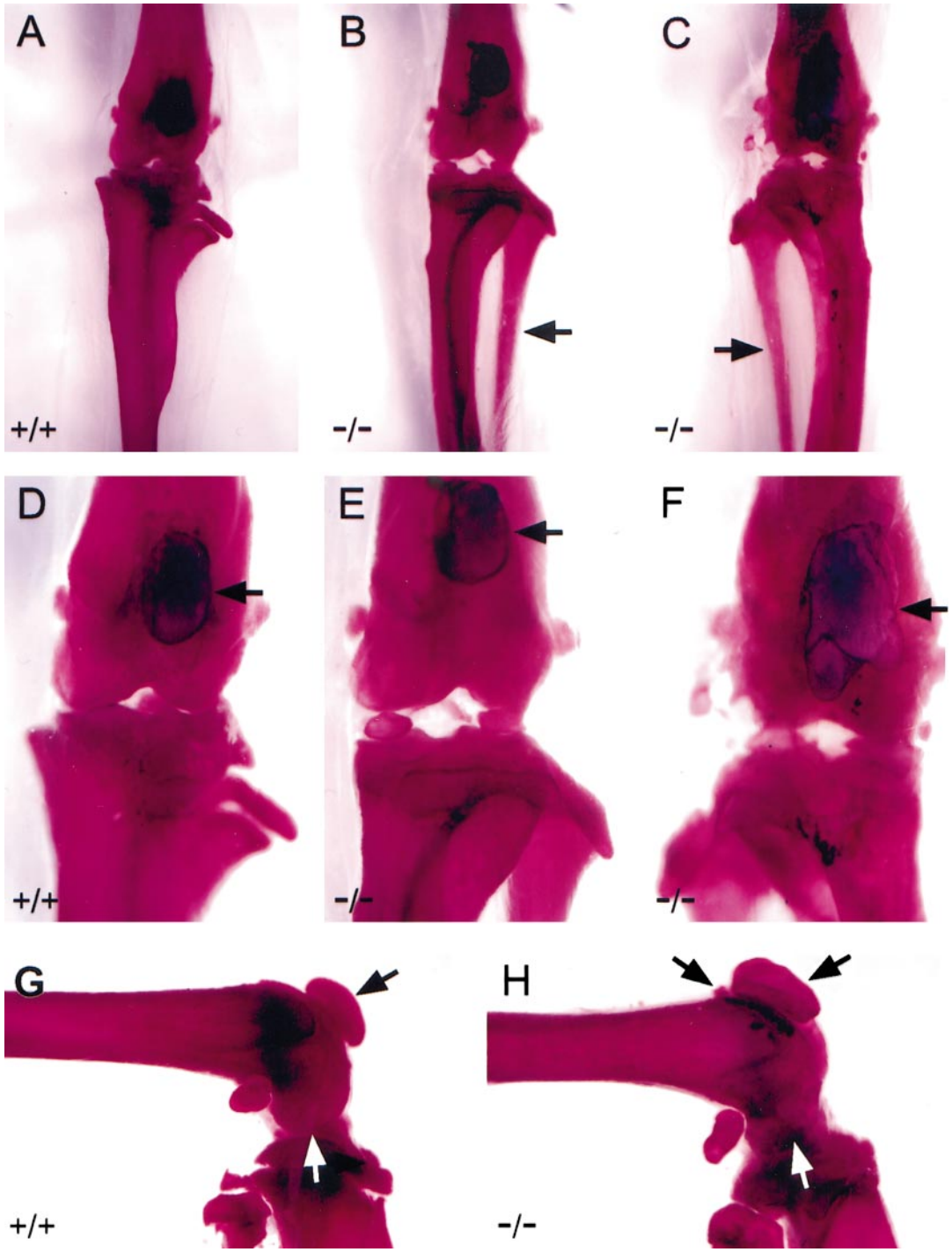

FIG. 4. Alterations in hindlimb skeletons in *Hoxd9/Hoxd10* mutant mice. Lower hindlimbs and knee joints of wild-type (A, D, and G) and mutant (B, C, E, F, and H) adult mice stained with alizarin red. (A) In wild-type mice when the femur is viewed from opposite the patella, the tibia is positioned in line with the femur such that the fibula is hidden from view. (B and C) In *Hoxd9/Hoxd10* mutant mice, when the femur is viewed from opposite the patella, the tibia is rotated to expose the underlying fibula. (D, E, and F) Higher magnification of the knee joints seen in A, B, and C. The mutant mouse in E has an expanded knee joint compared to the wild-type mouse in D. Younger mice (D and E) have smoother patellae (arrows in D and E) and sesamoid bones, whereas an older mutant (F) exhibits a more deteriorated and misshapen patella (arrow in F) and sesamoid bones. The mutant hindlimb in E also demonstrates a proximal shift of the patella along the femur. Lateral views of the knee joint in wild-type (G) and mutant (H) mice show the position of the patella (left-facing arrows). In H, the patella is shifted proximally and an anterior sesamoid bone is present at the proximal edge of the patella (right-facing arrow). White arrows in G and H indicate the articulation point.

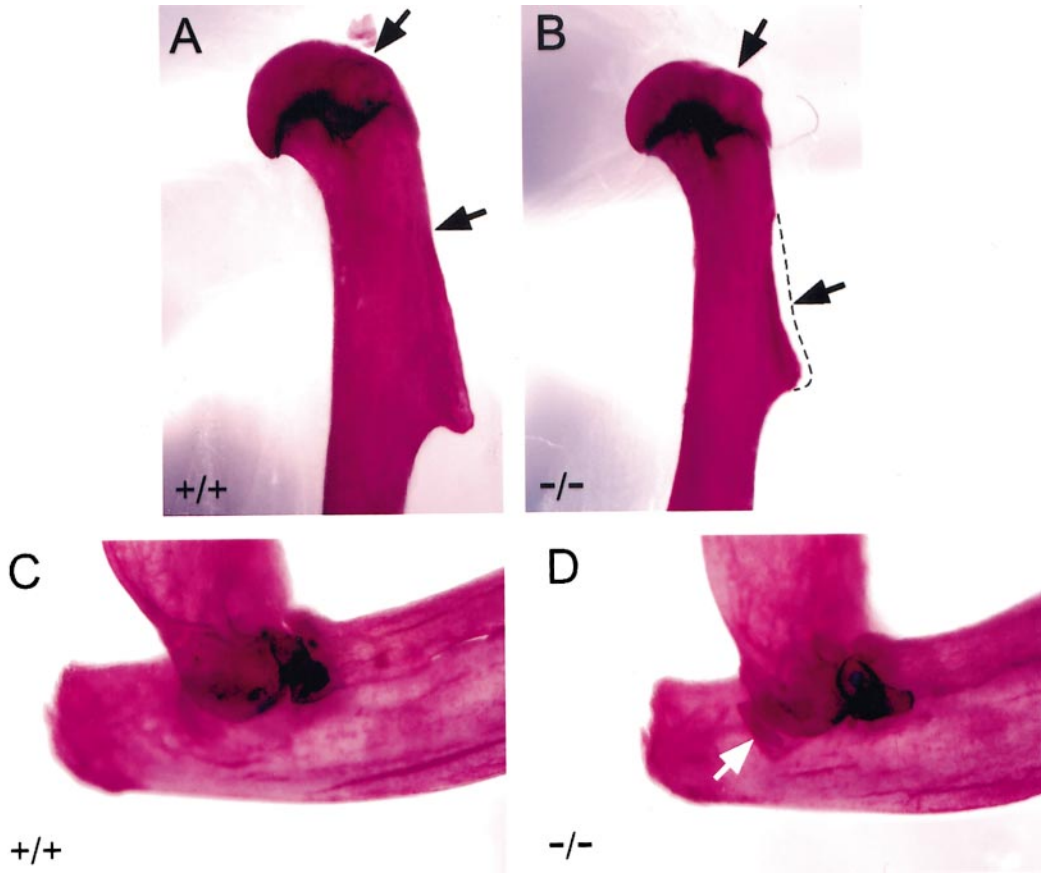

FIG. 5. Alterations in forelimb skeletons in *Hoxd9/Hoxd10* mutant mice. Lateral view of right humerus in wild-type (A) and *Hoxd9/Hoxd10* mutant (B) mice. Mutant mice have flatter humeral heads (upper arrow) and an underdeveloped deltoid crest (lower arrow). The profile of a wild-type deltoid crest is outlined over the mutant deltoid crest in (B). (C and D) Lateral view of the elbow in a wild-type (C) and mutant (D) animals. The arrow in D illustrates the presence of an ectopic sesamoid bone.

distal limb regions (Table 3). Mutant animals showed occasional deletions of single muscles in the medial and lateral regions of the distal hindlimb, while muscles in the anterior part of the limb were minimally affected. Most muscles, with the exception of peroneus brevis, appeared to be deleted in at least one animal, with flexor hallucis longus, peroneus tertius, fourth digit dorsolateral, and fifth digit lateral most often affected (Table 3). With the exception of the peroneus tertius muscle, all of medial and lateral region muscles were present in all wild-type hindlimbs examined. The variability in the presence of peroneus tertius may stem from its small size and close proximity to extensor digitorum longus (Marieb, 1995), which makes dissection and identification of this muscle difficult. In addition to muscle deletions, size reductions and misrouting of the distal tendons were also observed in mutant hindlimbs (Table 3).

Hoxd9/Hoxd10 mutant animals have kidneys which are reduced in size compared to wild-type littermates. Histological sections demonstrate a reduction in cross-sectional area of the kidney in both E15.5 embryos and newborn mice (data not shown). Mutant kidneys are approximately 70% the size of normal kidneys. However, histological organization of the kidneys appears unchanged in the mutants, with glomerular structure and positioning identical to that seen in wild-type animals. These alterations will be explored in greater detail elsewhere.

DISCUSSION

We have generated animals which carry a double mutation in the adjacent genes *Hoxd9* and *Hoxd10*. Mice which carry the double mutation show alterations in locomotor behavior, skeletal organization, peripheral nerve projections, and distal limb musculature. The observed phenotype in double-mutant mice is distinct from the phenotypes observed in mice carrying single mutations in either gene, but includes most of the features of both individual phenotypes. This suggests that these two genes may act both

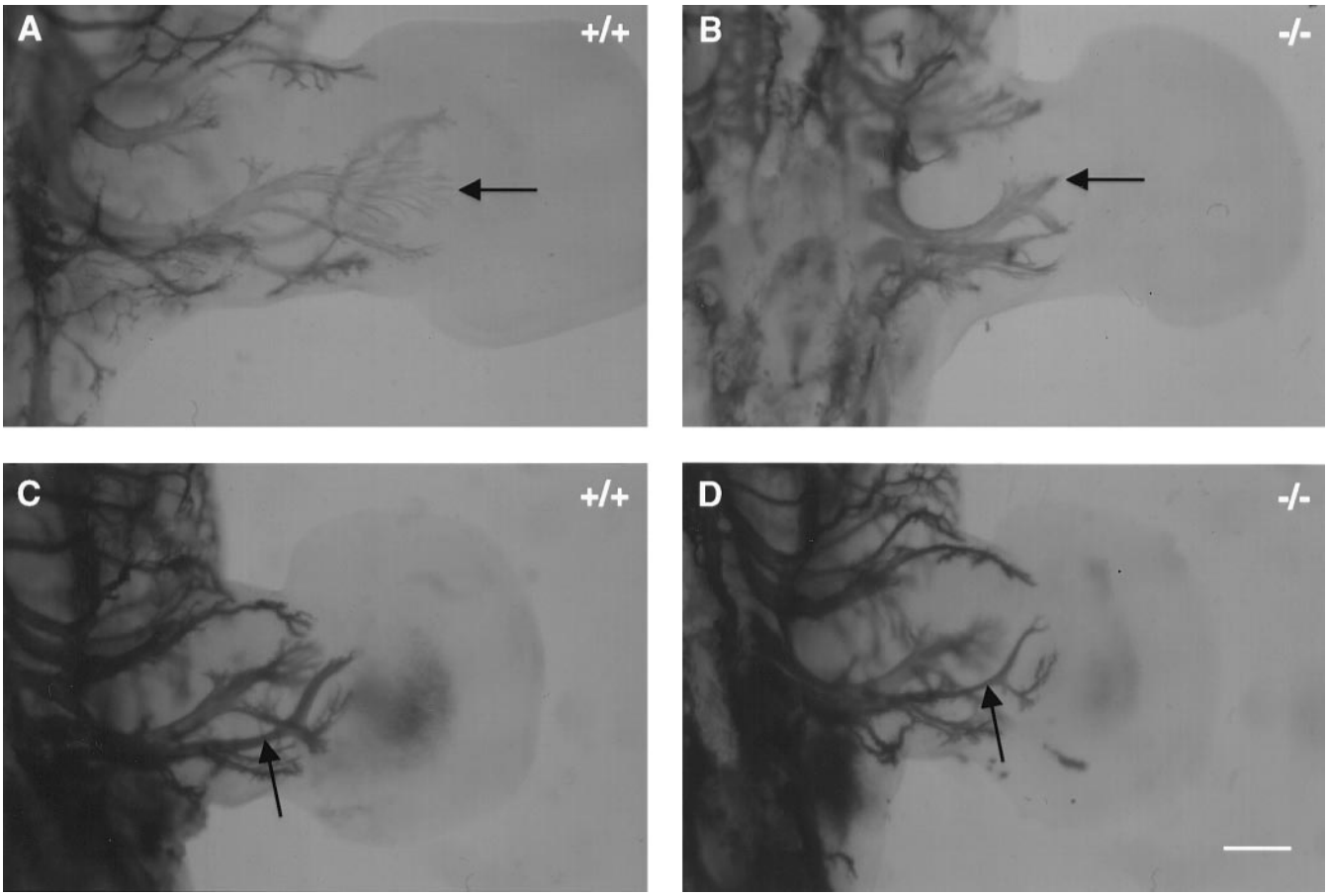

FIG. 6. Labeling with 2H3 anti-neurofilament antibody reveals the full extent of nerve projections into the hindlimbs of wild-type (A and C) and *Hoxd9/Hoxd10* mutant (B and D) littermate embryos at E12.5. The tibial nerve terminates in an expanded arbor in wild-type hindlimbs (arrow in A). In mutant embryos, the tibial nerve is truncated and the terminal arbor is missing (arrow in B). The deep peroneal nerve is robust and thick in wild-type embryos (arrow in C) but is reduced in diameter in mutant hindlimbs (arrow in D). Scale bar, 200 μm.

independently and in concert to pattern axial and appendicular structures in the developing embryo.

Locomotor Alterations Are Primarily Determined by Inactivation of Hoxd10

Disruption of *Hoxd9* and *Hoxd10* alters locomotor behavior by decreasing mobility and weight-bearing ability, changing the angle of foot placement and stride length, and eliminating hindlimb adduction. Alterations have also been reported for mice carrying a single mutation in the *Hoxd10* gene (Carpenter *et al.*, 1997); locomotor behavior appears to be normal in *Hoxd9* mutants (Fromental-Ramain *et al.*, 1996a). A similar distribution of gait defects was observed in *Hoxd10* single mutants and in *Hoxd9/Hoxd10* double mutants, with 59% of single mutants and 65% of double mutants demonstrating mild gait defects. There appeared to be a slight decrease in animals with severely affected gait in the double-mutant population (12% of double mutants compared to 17% of single mutants) and in both study populations a large number of animals exhibited loss of adduction (71% of double mutants and 86% of single mutants). These defects in locomotion are likely largely attributable to the mutation in *Hoxd10*, as there was no increase in severity or penetrance of the behavioral phenotype in the absence of *Hoxd9* activity, although loss of *Hoxd9* appears to increase the severity of peripheral nerve alterations, which might be expected to contribute to the behavioral phenotype. The observed decrease in severity in gait and adduction may stem from the difference between the induced mutations in *Hoxd10* single-mutant and *Hoxd9/Hoxd10* double-mutant animals. In single-mutant animals, *Hoxd10* was inactivated by insertion and retention of the *neo* gene; in double mutants the mutation is induced by a linker insertion with no incorporation of *neo.* This suggests that retention of *neo* in the *Hoxd10* single mutant may affect gene transcription or function as has been reported in other systems (Meyers *et al.*, 1998). One other

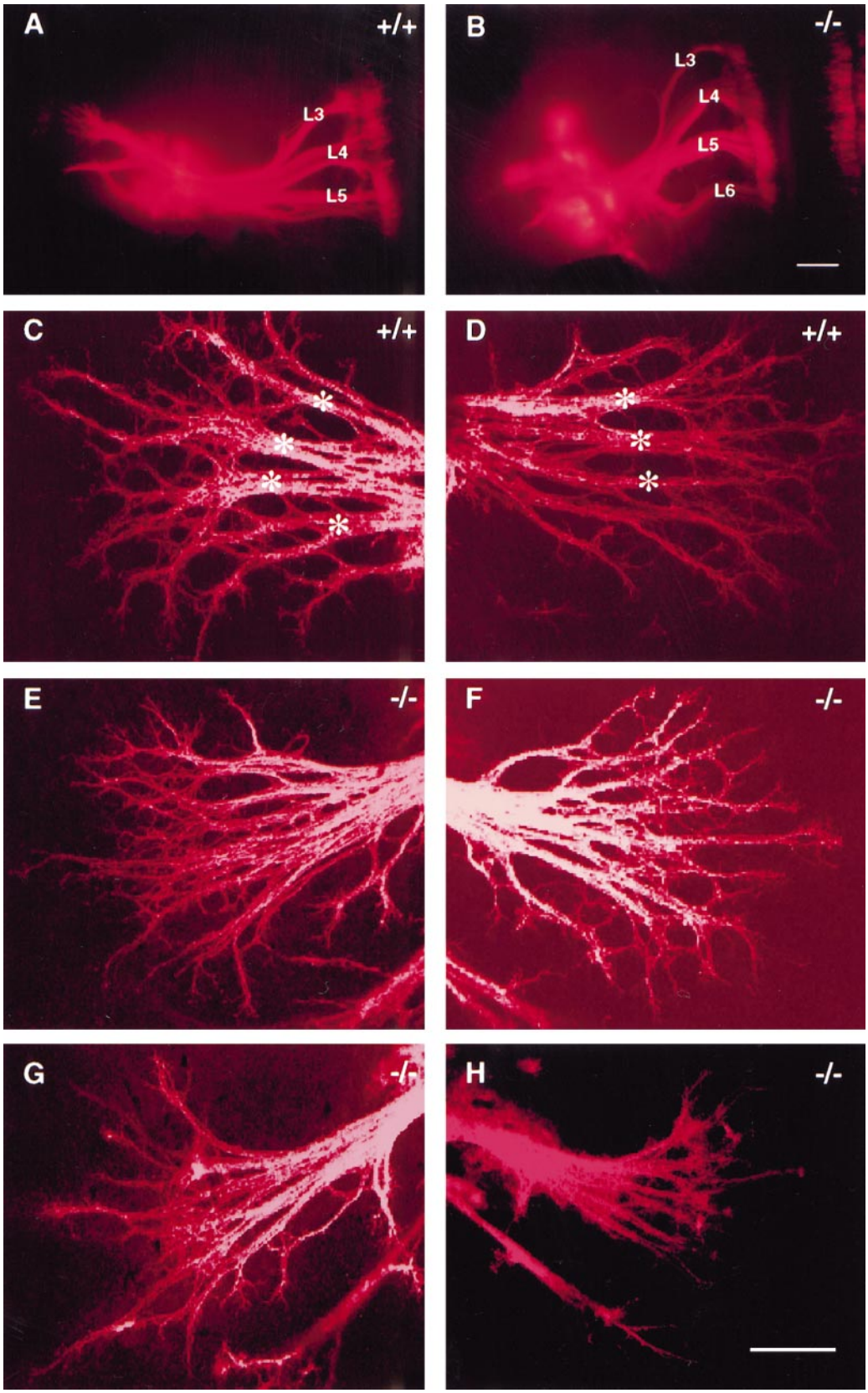

TABLE 3

Presence of Hindlimb Muscles and Nerves in *Hoxd9/Hoxd10* Mutant Mice

	Genotype	
	+/+	−/−
Muscles		
Anterior		
Extensor digitorum longus	6/6	18[a]/18
Tibialis anterior	6/6	18/18
Extensor hallucis longus	6/6	18[b]/18
Medial		
Flexor digitorum longus	6/6	17[c]/18
Tibialis posterior	6/6	17[c,d]/18
Flexor hallucis longus	6/6	15[c]/18
Lateral		
Peroneus brevis	6/6	18[a]/18
Peroneus longus	6/6	16/18
Peroneus tertius	2/6	7/18
4th digit dorsolateral	6/6	14/18
5th digit lateral	6/6	13[a]/18
Nerves		
Femoral	6/6	18/18
Saphenous	6/6	18/18
Sciatic	6/6	18[e]/18
Common peroneus	6/6	17[f]/18
Tibialis	6/6	18[b]/18

[a] Reduced in one hindlimb.
[b] Reduced in two hindlimbs.
[c] Tendon displaced medially in one hindlimb.
[d] Reduced in three hindlimbs.
[e] Branches into three nerves instead of two in one hindlimb.
[f] Reduced in 10 hindlimbs (extreme reduction in one hindlimb).

possibility is that the protein produced following the frameshift mutation is at least partially functional, although this seems unlikely given that the amino acid sequence changes completely downstream of the insertion and the protein is truncated 19 amino acids after the point of insertion.

Hoxd9 and Hoxd10 Induce Alterations in Axial and Appendicular Skeleton

Both *Hoxd9* and *Hoxd10* influence the development of the axial and appendicular skeleton. *Hoxd9* affects formation of lumbar and sacral vertebrae and the humerus (Fromental-Ramain *et al.,* 1996a), while *Hoxd10* affects the formation of the sacral vertebrae and the knee joint (Carpenter *et al.,* 1997). Double-mutant animals exhibit axial alterations only at the level of the sacral vertebrae. The vertebrae affected in the double-mutant animals are those which are individually affected in both of the single mutations, suggesting that vertebral transformations occurred only in regions of functional overlap between the two genes. One interesting observation is the lack of transformation of lumbar vertebrae. If *Hoxd9* and *Hoxd10* are acting independently, transformation of lumbar vertebrae would be an expected phenotype in the double-mutant animals, as this transformation is present in *Hoxd9* single mutants. Both *Hoxd9* and *Hoxd10* are expressed in the somitic mesoderm giving rise to lumbar vertebrae L3, L4, and L5, which are transformed in *Hoxd9* mutant animals (Fromental-Ramain *et al.,* 1996a). In *Hoxd9* mutant animals, *Hoxd10* expression would continue in this domain in the absence of *Hoxd9;* this *Hoxd10* expression may drive the anterior transformation of the lumbar vertebrae. In the absence of both *Hoxd9* and *Hoxd10,* other *Hox* genes, such as *Hoxa9* or *Hoxa10,* which are active in patterning lumbar but not sacral vertebrae (Favier *et al.,* 1996; Fromental-Ramain *et al.,* 1996a), may be able to compensate for *Hoxd9/Hoxd10* loss to establish the normal lumbar vertebral pattern.

The combined mutation affects components of the forelimb and hindlimb skeleton which are the normal domains of expression and effect for *Hoxd9* and *Hoxd10* individually and also produces a unique phenotype in the elbow. In the forelimb, mutation in *Hoxd9* alone produces a mild phenotype typified by a slight shortening of the humerus and remodeling of the deltoid crest (Fromental-Ramain *et al.,* 1996a). In *Hoxd9/Hoxd10* double mutants, the deltoid crest is reshaped, the head of the humerus is flattened, and ectopic lateral and ventral sesamoid bones are produced. Some of these latter phenotypes are also observed in *Hoxd9* mutants, but only in combination with an additional mutation in *Hoxa9* (Fromental-Ramain *et al.,* 1996a). These observations support a role for *Hoxd9* in skeletal patterning in the forelimb, but further demonstrate that this is a combinatorial role for *Hoxd9* and requires additional information provided either by *Hoxa9* or by *Hoxd10.* One alteration unique to *Hoxd9/Hoxd10* mutants is the production of an ectopic ventral sesamoid bone in the elbow; this

FIG. 7. Carbocyanine dye labeling of lumbar spinal nerves (A and B) and the distal portion of the tibial nerve (C–H) in wild-type (A, C, and D) and mutant (B, E, F, G, and H) embryos at E13.5. Retrograde dye transport from injections made at the base of the hindlimb labeled lumbar spinal nerves 3–5 (L3–L5) in a wild-type embryo (A). A similar injection in a mutant embryo labeled L3–L6 (B); the L3 projection appears much smaller in the mutant embryo. Labeling of the distal tibial nerve arbor in the right (C) and left (D) wild-type hindlimbs reveals condensed distinct axon fascicles (asterisks). Tibial arbors in right (E and G) and left (F and H) mutant hindlimbs show a broad range of phenotypes. E and F illustrate arbors which remain elongated but without discrete axon fascicles, whereas G and H show truncated arbors. Scale bar for A and B, 200 μm; for C–H, 50 μm.

phenotype may demonstrate a specific interaction between *Hoxd9* and *Hoxd10* which is not mirrored by the interaction between *Hoxa9* and *Hoxd9.* This phenotype also suggests that combinatorial mutations within the same linkage group can produce phenotypes which are greater than the sum of their individual components.

In the hindlimb, a mutation in *Hoxd10* remodels the knee joint and rotates the lower part of the limb (Carpenter *et al.,* 1997). Similar alterations are observed in the double mutant with a characteristic shift in the patella and production of ectopic anterior sesamoid bones shared between the single and the double mutation. Rotation of the lower part of the limb is more prevalent in *Hoxd10* single mutants (63% compared to 26% of double mutants). This lesser degree of limb rotation is reflected in the behavioral observations in that 71% of double-mutant mice demonstrated loss of adduction compared to 86% of single mutants. Rotation of the lower part of the limb is likely to contribute significantly to this defect, although it is not the only contributor as rotation was observed in only 26% of *Hoxd9/Hoxd10* hindlimbs, yet adduction defects were observed in 71% of double-mutant animals. This lesser degree of rotation may also be due to differences in gene activity due to the inclusion of *neo* in the single mutation and its exclusion from *Hoxd10* in the double mutation. One unique aspect of the hindlimb phenotype is the occasional fragmented appearance of the patella. Similar observations on elbow sesamoid bones were made in *Hoxa9/Hoxd9* double mutants (Fromental-Ramain *et al.,* 1996a). This fragmentation may reflect secondary ossification due to impaired joint mobility or may reflect alterations in chondrogenesis and ossification induced by alterations in *Hox* gene activity.

Hoxd9/Hoxd10 Mutations Produce Alterations in Peripheral Nerve Patterning

Inactivation of *Hoxd9* and *Hoxd10* produces alterations in spinal and peripheral nerves, including a reduction in size of the L3 spinal nerve, truncation of the distal tibial nerve arbor, and reduction in the size of the deep peroneal nerve. These alterations may all stem from changes in the motor neuron population of the L3 spinal segment. Motor neurons positioned in L3 normally project out of the spinal cord through the L3 spinal nerve. Some of the motor neurons which project into the tibial and peroneal nerves are located in this segment (McHanwell and Biscoe, 1981); the peripheral projections from these motor pools appear to be specifically affected in *Hoxd9/Hoxd10* mutants. Similar alterations are also observed in *Hoxd10* mutants (Carpenter *et al.,* 1997), with no reported alterations in central or peripheral nerve patterning in *Hoxd9* mutant animals. *Hoxd10* mutants show a reduction in the number of spinal cord segments providing hindlimb innervation through the sacral plexus and alterations in the peripheral projections made by motor neurons which normally reside in this segment, suggesting an anterior transformation of the L3 spinal segment to an L2-like identity (Carpenter *et al.,* 1997). Alterations in the L3 spinal nerve and its peripheral projections appear similar in both single and double mutants, suggesting that L3 is transformed to an L2 identity in the double-mutant embryos as well. However, the severity of the peripheral nerve alterations appears increased in double-mutant embryos. The number of nerve fibers in the tibial arbor is reduced in both types of embryos, but the alterations in the double mutants appear more extreme in that the entire arbor appears truncated in 36% of animals and the fasciculation and branching patterns of the nerve arbor appear to be affected. In *Hoxd10* single-mutant animals, the peroneal nerve was reduced in 20% of adult animals and missing in 30% of embryos examined (Carpenter *et al.,* 1997), while in double-mutant animals, the peroneal nerve was reduced or missing in 61% of adult hindlimbs and reduced in diameter in all embryos examined. Our previous observations had suggested that inactivation of *Hoxd10* affected peripheral nerve projections into the hindlimb (Carpenter *et al.,* 1997); the increase in prevalence and severity of tibial and peroneal nerve alterations suggest that *Hoxd9* and *Hoxd10* act in concert to pattern hindlimb peripheral nerve projections. Functional integrity of *Hoxd9* and *Hoxd10* may be required to activate genes required for motor neuron generation or specification or genes required in axonal pathfinding; future studies will be directed at uncovering the identity of genes which are regulated by *Hoxd9* and *Hoxd10* independently and together.

Inactivation of single *Hox* genes produces clear effects on the development of the nervous system. In particular, *Hox* gene disruption affects motor neuron development and efferent projections from the CNS at the level of the hindbrain and spinal cord (Carpenter *et al.,* 1993, 1997; Mark *et al.,* 1993; Goddard *et al.,* 1996; Tiret *et al.,* 1998). Disruption of multiple paralogous genes produces more pronounced alterations in the nervous system than disruption of single genes (Gavalas *et al.,* 1998; Studer *et al.,* 1998), supporting the hypothesis that combinatorial *Hox* gene activity is required to pattern the nervous system. However, combinatorial function of genes positioned within the same *Hox* linkage group on the nervous system has only been briefly examined (Rancourt *et al.,* 1995). Our current observations suggest that combinatorial activity between *Hox* genes in the same linkage group may also be required for nervous system patterning. In particular, the combined activity of *Hoxd9* and *Hoxd10* is needed for proper outgrowth and patterning of hindlimb peripheral nerves.

Our observations on *Hoxd9/Hoxd10* double-mutant animals support the idea that functional interactions between adjacent members of the same *Hox* linkage group are required for proper development of mouse embryos. Previous observations have demonstrated combinatorial effects of *Hoxd11, Hoxd12,* and *Hoxd13* on skeletal patterning (Davis and Capecchi, 1996; Zakany and Duboule, 1996); our studies have demonstrated alterations in axial and appendicular skeleton, hindlimb musculature, and the peripheral

nervous system in *Hoxd9/Hoxd10* double-mutant animals. Our observations demonstrate a large degree of overlap with the phenotypes of single-mutant animals, but with significant differences in both structure and severity which suggest that the two genes do not act entirely independently. Therefore, a variety of *Hox* gene interactions, both within and between linkage groups, may be required to properly pattern a developing embryo.

ACKNOWLEDGMENTS

We thank Dr. Mario Capecchi for advice and encouragement during the initial stages of this project, Lorraine Baynosa and Sarah Buxton for excellent technical assistance, and Michael Levine for providing access to the confocal microscope. The 2H3 hybridoma supernatant was obtained from the Developmental Studies Hybridoma Bank under Contract N01-HD-6-2915 from the NICHD. These studies were funded by a UCLA Frontiers of Science Faculty Research Award to E.M.C.

REFERENCES

Bensen, G. V., Lim, H., Paria, B. C., Satokata, I., Key, S. K., and Maas, R. L. (1996). Mechanisms of reduced fertility in *Hoxa-10* mutant mice: Uterine homeosis and loss of maternal *Hoxa-10* expression. *Development* **122,** 2687–2696.

Boulet, A. M., and Capecchi, M. R. (1996). Targeted disruption of *hoxc-4* causes esophageal defects and vertebral transformations. *Dev. Biol.* **177,** 232–249.

Bürglin, T. R. (1994). A comprehensive classification of homeobox genes. *In* "Guidebook to the Homeobox Genes" (D. Duboule, Ed.), pp. 27–71. Oxford Univ. Press, New York.

Carpenter, E. M., Goddard, J. M., Chisaka, O., Manley, N. R., and Capecchi, M. R. (1993). Loss of *Hox-A1* (*Hox-1.6*) function results in the reorganization of the murine hindbrain. *Development* **118,** 1063–1075.

Carpenter, E. M., Goddard, J. M., Davis, A. P., Nguyen, T. P., and Capecchi, M. R. (1997). Targeted disruption of *Hoxd-10* affects mouse hindlimb development. *Development* **124,** 4505–4514.

Condie, B. G., and Capecchi, M. R. (1993). Mice homozygous for a targeted disruption of *Hoxd-3* (*Hox-4.1*) exhibit anterior transformation of the first and second cervical vertebrae, the atlas and the axis. *Development* **119,** 579–595.

Condie, B. G., and Capecchi, M. R. (1994). Mice with targeted disruptions in the paralogous genes *hoxa-3* and *hoxd-3* reveal synergistic interactions. *Nature* **370,** 304–307.

Davis, A. P., and Capecchi, M. R. (1994). Axial homeosis and appendicular skeleton defects in mice with a targeted disruption of *hoxd-11*. *Development* **120,** 2187–2198.

Davis, A. P., and Capecchi, M. R. (1996). A mutational analysis of the 5′ *HoxD* genes: Dissection of genetic interactions during limb development in the mouse. *Development* **122,** 1175–1185.

Davis, A. P., Witte, D. P., Hsieh-Li, H. M., Potter, S. S., and Capecchi, M. R. (1995). Absence of radius and ulna in mice lacking *hoxa-11* and *hoxd-11*. *Nature* **375,** 791–795.

Dollé, P., Dierich, A., LeMeur, M., Schimmang, T., Schuhbaur, B., Chambon, P., and Duboule, D. (1993). Disruption of the *Hoxd-13* gene induces localized heterochrony leading to mice with neotenic limbs. *Cell* **75,** 431–441.

Dollé, P., Izpisúa-Belmonte, J.-C., Falkenstein, H., Renucci, A., and Duboule, D. (1989). Coordinate expression of the murine *Hox-5* complex homeobox-containing genes during limb pattern formation. *Nature* **342,** 767–772.

Favier, B., Le Meur, M., Chambon, P., and Dollé, P. (1995). Axial skeleton homeosis and forelimb malformations in *Hoxd-11* mutant mice. *Proc. Natl. Acad. Sci. USA* **92,** 310–314.

Favier, B., Rijli, F. M., Fromental-Ramain, C., Fraulob, V., Chambon, P., and Dollé, P. (1996). Functional cooperation between the non-paralogous genes *Hoxa-10* and *Hoxd-11* in the developing forelimb and axial skeleton. *Development* **122,** 449–460.

Fromental-Ramain, C., Warot, X., Lakkaraju, S., Favier, B., Haack, H., Birling, C., Dierich, A., Dollé, P., and Chambon, P. (1996a). Specific and redundant functions of the paralogous *Hoxa-9* and *Hoxd-9* genes in forelimb and axial skeleton patterning. *Development* **122,** 461–472.

Fromental-Ramain, C., Warot, X., Messadecq, N., LeMeur, M., Dollé, P., and Chambon, P. (1996b). *Hoxa-13* and *Hoxd-13* play a crucial role in the patterning of the limb autopod. *Development* **122,** 2997–3011.

Gaunt, S. J., Krumlauf, R., and Duboule, D. (1989). Mouse homeogenes within a subfamily, Hox-1.4, -2.6 and -5.1, display similar anteroposterior domains of expression in the embryo, but show stage- and tissue-dependent differences in their regulation. *Development* **107,** 131–141.

Gavalas, A., Studer, M., Lumsden, A., Rijli, F., Krumlauf, R., and Chambon, P. (1998). *Hoxa1* and *Hoxb1* synergize in patterning the hindbrain, cranial nerves and second pharyngeal arch. *Development* **125,** 1123–1136.

Goddard, J. M., Rossel, M., Manley, N. R., and Capecchi, M. R. (1996). Mice with targeted disruption of *Hoxb-1* fail to form the motor nucleus of the VIIth nerve. *Development* **122,** 3217–3228.

Izpisúa-Belmonte, J.-C., Falkenstein, H., Dollé, P., Renucci, A., and Duboule, D. (1991). Murine genes related to the *Drosophila AbdB* homeotic gene are sequentially expressed during development of the posterior part of the body. *EMBO J.* **10,** 2279–2289.

Mansour, S. L., Goddard, J. M., and Capecchi, M. R. (1993). Mice homozygous for a targeted disruption of the proto-oncogene *int-2* have developmental defects in the tail and inner ear. *Development* **117,** 13–28.

Mansour, S. L., Thomas, K. R., and Capecchi, M. R. (1988). Disruption of the proto-oncogene *int-2* in mouse embryo-derived stem cells: A general strategy for targeting mutations to nonselectable genes. *Nature* **336,** 348–352.

Marieb, E. N. (1995). "Human Anatomy and Physiology." Benjamin/Cummings, Redwood City, CA.

Mark, M., Lufkin, T., Vonesch, J.-L., Ruberte, E., Olivo, J.-C., Dollé, P., Gorry, P., Lumsden, A., and Chambon, P. (1993). Two rhombomeres are altered in *Hoxa-1* mutant mice. *Development* **119,** 319–338.

McHanwell, S., and Biscoe, T. J. (1981). The localization of motoneurons supplying the hindlimb muscles of the mouse. *Philos. Trans. R. Soc. London B* **293,** 477–508.

Meyers, E. N., Lewandowski, M., and Martin, G. R. (1998). An *Fgf8* mutant allelic series generated by Cre- and Flp-mediated recombination. *Nat. Genet.* **18,** 136–141.

Rancourt, D. E., Tsuzuki, T., and Capecchi, M. R. (1995). Genetic interaction between *hoxb-5* and *hoxb-6* is revealed by nonallelic noncomplementation. *Genes Dev.* **9,** 108–122.

Renucci, A., Zappavigna, V., Zákány, J., Izpisúa-Belmonte, J. C., Bürki, K., and Duboule, D. (1992). Comparison of mouse and

human HOX-4 complexes defines conserved sequences involved in the regulation of *Hox-4.4*. *EMBO J.* **11,** 1459–1468.

Rijli, F. M., and Chambon, P. (1997). Genetic interactions of *Hox* gene in limb development: Learning from compound mutants. *Curr. Opin. Genet. Dev.* **7,** 481–487.

Rijli, F. M., Matyas, R., Pellegrini, M., Dierich, A., Gruss, P., Dollé, P., and Chambon, P. (1995). Cryptorchidism and homeotic transformations of spinal nerves and vertebrae in *Hoxa-10* mutant mice. *Proc. Natl. Acad. Sci. USA* **92,** 8185–8189.

Satokata, I., Bensen, G., and Maas, R. (1995). Sexually dimorphic sterility phenotypes in *Hoxa10*-deficient mice. *Nature* **374,** 460–463.

Studer, M., Gavalas, A., Marshall, H., Ariza-McNaughton, L., Rijli, F. M., Chambon, P., and Krumlauf, R. (1998). Genetic interactions between *Hoxa1* and *Hoxb1* reveal new roles in regulation of early hindbrain patterning. *Development* **125,** 1025–1036.

Tang, J., Rutishauser, U., and Landmesser, L. (1994). Polysialic acid regulates growth cone behavior during sorting of motor axons in the plexus region. *Neuron* **13,** 405–414.

Thomas, K. R., and Capecchi, M. R. (1987). Site-directed mutagenesis by gene targeting in mouse embryo-derived stem cell. *Cell* **51,** 503–512.

Thomas, K. R., and Capecchi, M. R. (1990). Targeted disruption of the murine *int-1* proto-oncogene resulting in severe abnormalities in midbrain and cerebellar development. *Nature* **346,** 847–850.

Tiret, L., Le Mouellic, H., Maury, M., and Brûlet, P. (1998). Increased apoptosis of motoneurons and altered somatotopic maps in the brachial spinal cord of *Hoxc-8*-deficient mice. *Development* **125,** 279–291.

Zákány, J., and Duboule, D. (1996). Synpolydactyly in mice with a targeted deficiency in the *HoxD* complex. *Nature* **384,** 69–71.

Received for publication August 12, 1999
Revised October 5, 1999
Accepted October 5, 1999